Cooperativity in Ion Hydration

K.J. Tielrooij, N. Garcia-Araez, M. Bonn, and H.J. Bakker*

FOM Institute for Atomic and Molecular Physics [AMOLF]
Science Park 104, 1098 XG Amsterdam, The Netherlands

Despite prolonged scientific efforts to unravel the effects of ions on the structure and dynamics of water, many open questions remain, in particular concerning the spatial extent of this effect (how many water molecules are affected) and the origin of ion-specific effects. A combined terahertz and femtosecond infrared spectroscopic study of water dynamics around different ions (specifically magnesium, lithium, sodium and cesium cations, as well as sulfate, chloride, iodide and perchlorate anions) reveals that the effect of ions and counterions on water can be strongly interdependent and non-additive, and in certain cases extends well beyond the first solvation shell of water molecules directly surrounding the ion.

The properties of solutions of ions in water are of relevance for a wide range of systems, including biological environments [1] and atmospheric aerosols [2]. Interestingly, even for simple binary solutions the effect of ions on the structure and dynamics of water has been the subject of ongoing debate [3–5]. Key questions concerning ion effects on water pertain to the number of water molecules that are affected, and how the different degrees of freedom of these water molecules are influenced.

During the last decade a variety of measurement techniques has provided evidence that ions primarily have an effect on the structure and dynamics of the first solvation shell of water molecules directly surrounding the ion. This evidence consists of structural measurements of ion hydration using neutron and X-ray diffraction [6, 7], X-ray absorption spectroscopy [8] and infrared and Raman spectroscopy [9]. Information on the ion effects on water dynamics has been mainly obtained from femtosecond time-resolved infrared vibrational spectroscopy (fs-IR) [10–12] and optical Kerr effect spectroscopy [13]. These reports support the notion that the effect of ions on water is largely limited to the first solvation shell. A different dynamical technique, dielectric relaxation (DR), also showed that for many different cations and anions, the effect is limited to the first solvation shell [14–17]. However, for certain ion combinations an effect beyond the first solvation shell was observed [18–20]. It is currently unclear what factors determine the degree of hydration and what constitutes the molecular level structure and dynamics: a unifying molecular picture of ion hydration is lacking.

Here, we study the effect of ions on water using femtosecond vibrational infrared spectroscopy (fs-IR) and terahertz dielectric relaxation (DR). It turns out that these techniques are uniquely complementary, in that they are sensitive to water reorientation dynamics along different molecular axes of water. Moreover, the ability to independently resolve water reorientation along different directions helps to uncover previously unappreciated cooperativity between hydrated cations and anions. We study dissolved salts, containing various combinations of ions that have different charge densities and water affinities. For specific combinations of cations and anions we observe dynamic hydration effects that extend well beyond the first structural solvation shell.

We first present the results of DR spectroscopy of five different dissolved salts A1. These measurements were performed by characterizing in time the propagation of a terahertz (THz) pulse, with a duration of $\sim$1 ps through the salt solution. In the inset of Fig. A, we show THz pulses as transmitted through 0.5 mol/kg solutions of Cs_2SO_4, $MgSO_4$ and through a reference solution of CsCl [16]. Generally, THz pulses are delayed as a result of refraction and experience a decrease in amplitude as a result of absorption. In water, a marked frequency dependence of refraction and absorption arises when the dipoles of water molecules fail to keep up reorienting with an externally applied oscillating electric field. This process is called dielectric relaxation (DR) and leads to a large absorption peak at 20 GHz and a smaller one around 0.6 THz, for pure water molecules at room temperature. These peaks are attributed to the collective reorientation of water molecules ($\tau_D \approx 8$ ps) and the reorientation of undercoordinated water molecules ($\tau_2 \approx 250$ fs), respectively [21, 22]. In Fig. A, we show the imaginary part of the extracted dielectric function ϵ, which is associated with absorption of electromagnetic radiation by water molecules. As a result of the interaction with solvated ions, the reorientation of water molecules around ions slows down, shifting the absorption peak to lower frequencies and thereby reducing the absorption of radiation at THz frequencies (depolarization).

It is typically found that the dynamics of water molecules in salt solutions are non-uniform and show two or more time scales. In previous dielectric relaxation studies it is observed that a certain number of water molecules shows very slow reorientation dynamics, whereas for the remaining water molecules the orientational dynamics are similar to bulk liquid water [14–20]. Also in computer simulations it is found that a fraction of water remains that is unaffected by the presence of

---

the ions [23, 24]. In analyzing the THz data, we follow the literature by identifying two sub-ensembles of water molecules in ionic solution: those whose dynamics are predominantly unaffected by the presence of ions, and those whose dynamics are slowed down. Both sub-ensembles are characterized by a distribution of reorientation time scales.
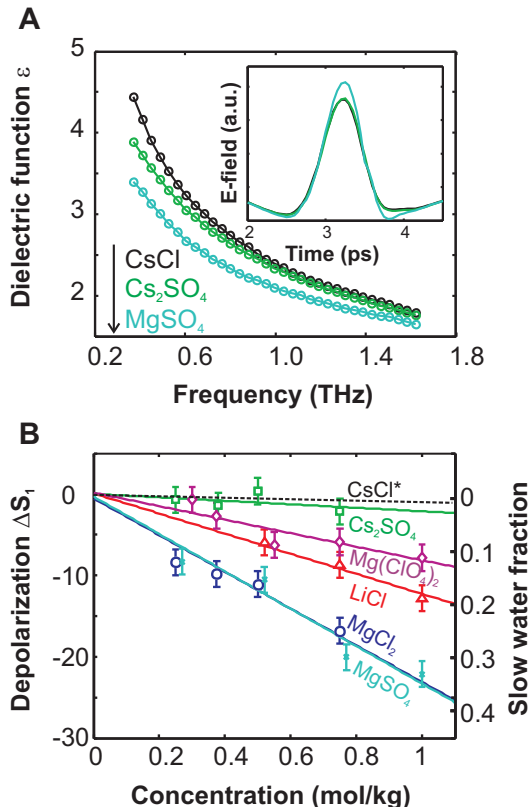

FIG. 1: Results of DR spectroscopy. **(A)** The imaginary part of the dielectric function ϵ for 0.5 mol/kg solutions of CsCl, Cs_2SO_4 and $MgSO_4$ and the corresponding transmitted THz pulses (inset). **(B)** The depolarization (corrected for kinetic depolarization due to conductivity [21]) and fraction of slow water as a function of concentration for the investigated salt solutions. The fraction of slow water is equal to the depolarization divided by the difference between the dielectric response of pure water at zero and infinite frequency, which equals 74 at 298 K. The lines are linear fits to the depolarization values/slow fractions and serve to distinguish the studied salts. Error bars represent the 95% confidence interval and are derived through error propagation of the experimental uncertainty in the dielectric function. *Data from Ref. [16].

In Fig. B, we show the concentration-dependent depolarization and corresponding slow water fraction. The hydration number $N_{\vec{p}}$ is defined as the number of moles of slow water dipoles ($\vec{p}$) per mole dissolved salt and is directly proportional to the slopes of the lines in Fig. B [14–20]. The hydration number is a dynamical property and is therefore distinct from the structural concept of solvation shells. Solvation shells are often defined in terms of the distance distribution of the water molecules from the center of the ion, but as such do not present information on the dynamics of the water molecules. It is typically found that ions with a larger charge density (small, multivalent ions) affect the dynamics of a larger number of water molecules, i.e. have a higher hydration number, than ions with a lower charge density (large, monovalent ions) [6, 7, 14–16, 18–20]. This is caused by the larger local electric field around these ions, which affects the orientation of a larger number of surrounding water molecules. Our results for $MgCl_2$, LiCl and CsCl are in good agreement with this general rule. For $Mg(ClO_4)_2$ we find $N_{\vec{p}} = 6$, and as ClO_4^- is a very weakly hydrated anion, the observed slowly reorienting water molecules are likely located in the first geometrically surrounding solvation shell of the Mg^{2+} ion. In contrast, for Cs_2SO_4 $N_{\vec{p}}$ is only 1. Apparently, the water molecules in the solvation shell of Cs^+ show reorientational dynamics similar to bulk liquid water [16], probably because the positive charge of the Cs^+ ion is distributed over a large volume: The slowly reorienting water can be attributed to a water molecule located within the solvation shell of strongly hydrated SO_4^{2-}, presumably forming hydrogen bonds with both OH groups to two oxygen atoms of the SO_4^{2-} ion. The low value of $N_{\vec{p}}$ found for Cs_2SO_4 indicates that the effect of anions on water reorientation is either negligible or not measurable by DR measurements. Similarly, a previous GHz DR measurement of the anions Br^-, I^-, NO_3^-, ClO_4^- and SCN^- found that the impact of these anions on water dynamics is remarkably small and remarkably similar, despite the different water affinities of these ions [17].

Complementary to DR measurements, we use femtosecond time-resolved infrared vibrational spectroscopy (fs-IR) measurements A1. This technique allows the direct study of the reorientational dynamics of individual water molecules with high temporal resolution ($\sim$150 fs). In these experiments, we excite the OD-stretch vibration of a subset of HDO molecules in H_2O (4% D_2O in H_2O). Molecules with their OD-group preferentially aligned along the polarization axis of the excitation (pump) pulse are most efficiently tagged. By interrogating, using a second laser (probe) pulse, the number of tagged molecules parallel and perpendicular to the excitation axis, the rotation of tagged molecules can be followed in time. The anisotropy $R(t)$ (corrected for heating due to the excitation according to Ref. [25]) as a function of pump-probe delay time t reflects the orientational dynamics of the probed water molecules. For bulk water, the decay of $R(t)$ is directly related to the reorientation time τ_D, as measured by DR spectroscopy [26]. Figures A-C show the anisotropy decay for the dissolved salts $Mg(ClO_4)_2$, Cs_2SO_4 and $MgSO_4$, each for concentrations ranging from 0 to 2 mol/kg. A remarkable conclusion can be drawn from these three measurements: $MgSO_4$ shows a very large
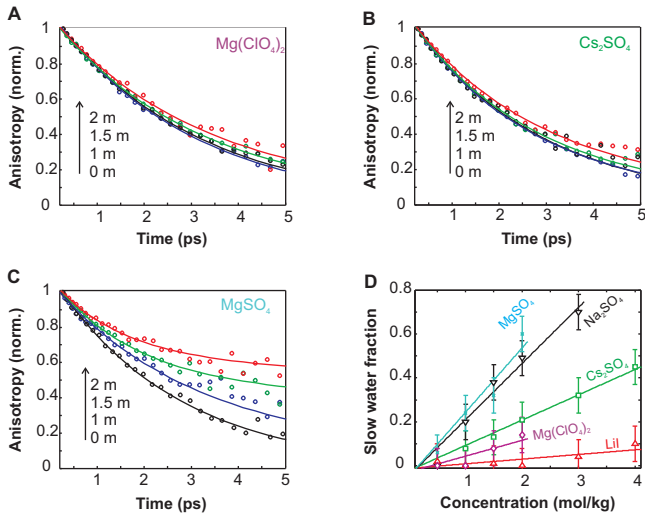
FIG. 2: Results of fs-IR spectroscopy. The normalized decay of the anisotropy $R(t)$ for a number of concentrations of $Mg(ClO_4)_2$ (**A**), Cs_2SO_4 (**B**) and $MgSO_4$ (**C**). We fit the anisotropy decay of all different salt solutions using double exponentials with floating amplitudes and fixed time scales: a time scale of 2.6 ps, as in bulk water [25], and a slow water time scale of 10 ps. (**D**) The fraction of slow water compared to bulk-like water. The lines are linear fits and serve as guides to the eye to distinguish the studied salts. The error bars are based on at least four measurement runs and represent the 95% confidence interval.

slow reorientation component, whereas Mg^{2+} and SO_4^{2-} individually, in combination with other ions (ClO_4^- and Cs^+, resp.) do not. This shows that the effect of ions on water dynamics can be non-additive, which will be discussed in detail later on in this report. First, we focus our attention on the observation that there is an apparent discrepancy between the DR measurements and the fs-IR measurements. For hydrated cations, DR and fs-IR give different results: Mg^{2+} and Li^+ show large immobilized fractions when measured with DR, but the fs-IR measurements of $Mg(ClO_4)_2$ and LiI show complete reorientation, with a negligible slow fraction (see Fig. D). These fractions have been obtained using a bimodal model, analogous to the DR measurements: the slow time constant and the associated fraction of hydration water are obtained from a double exponential fit to the anisotropy decay, in which the fast time constant equals the reorientation time constant of 2.6 ps of pure water. This fast time constant is determined in an independent measurement on pure water. The slow component represents a weighted average of water molecules that have in common that they reorient much more slowly than the water molecules in bulk liquid water. Here it should be noted that the exchange of water molecules between the dynamic hydration shells and the bulk typically takes place on a time scale of tens to hundreds of picoseconds [27]. This exchange time scale is much longer than the reorientation time of

~2.6 ps of bulk liquid water. Hence the reorientation of the water molecules outside the dynamic hydration shells is well separated from the reorientation dynamics of the water molecules in the dynamic hydration shells. In analogy to the DR measurements, the slow water fraction as measured with fs-IR can be translated into a hydration number $N_{\vec{\mu}}$. This corresponds to the number of moles of slowly reorienting OH-groups (with transition dipole moment $\vec{\mu}$) per mole dissolved salt (keeping in mind that there are two OH-groups per water molecule).
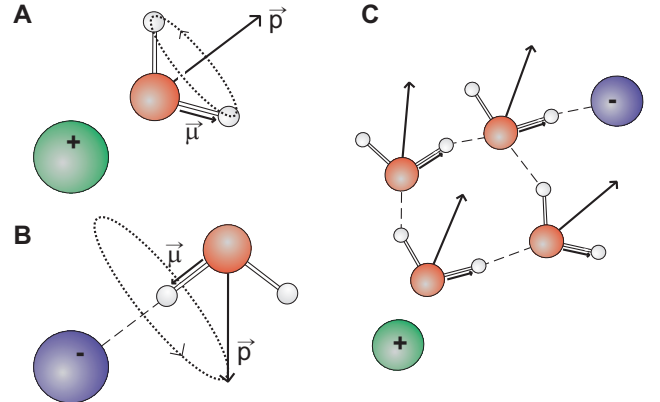

FIG. 3: Semi-rigid hydration and cooperativity. A water molecule in the solvation shell of a cation (**A**) and an anion (**B**). Dielectric relaxation measurements probe the reorientation of the permanent dipole vector $\vec{p}$. Femtosecond infrared spectroscopy is sensitive to the reorientation of the OD-stretch transition dipole moment $\vec{\mu}$. The dotted arrows indicate reorientation in a cone, in the case of semi-rigid hydration. **C** Proposed geometry, in which the water dynamics are locked in two directions due to the cooperative interaction with the cation and the anion.

The differences between the results of DR and fs-IR can be understood by noting the different vectors that the two measurement techniques probe: the permanent dipole moment of water molecules $\vec{p}$ in the case of DR and the OD-stretch transition dipole moment $\vec{\mu}$ in the case of fs-IR (see Fig. 3). The local electric field around the ions causes the dipole vector $\vec{p}$ of water molecules in the solvation shell of a cation to point radially away from the cation, whereas for an anion one of the OH-groups of a hydrogen-bonded water molecule linearly points towards the anion [9, 28]. From Fig. 3, it is clear that there is rotational motion of water molecules in the cationic solvation shell, which does not lead to reorientation of the vector $\vec{p}$, but does result in randomization of the transition dipole vector $\vec{\mu}$. For the case of anions, the reverse effect occurs: for water molecules in the anionic solvation shell, the motion of $\vec{p}$ is unrestricted within a cone with fixed axis $\vec{\mu}$, where $\vec{\mu}$ is the OD-bond that is hydrogen-bonded to the anion. Reorientation in a cone with a semi-cone angle between $\vec{\mu}$ and $\vec{p}$ of $\alpha \approx 52°$ (half the HOD-bond angle) leads to a complete randomization of the vector whose motion is unrestricted within the cone A1. This

explains the insensitivity of DR towards anionic, and of fs-IR towards cationic, hydration. For both cations and anions, these observations lead to a molecular picture of semi-rigid hydration, i.e. water molecules in ionic solvation shells that reorient in a propeller-like manner, giving rise to partial reorientation, along a distinct axis.

The molecular picture of semi-rigid hydration explains the ion effect on water molecules directly surrounding the ion. This picture holds for salts for which one of the counterions is weakly hydrated. However, when both ions are strongly hydrated, the effect on water dynamics can be much stronger and non-additive. The THz DR data show that $Mg(ClO_4)_2$ has a hydration number $N_{\vec{p}} = 6$ and that Cs_2SO_4 has a hydration number $N_{\vec{p}} = 1$, respectively associated with water molecules directly adjacent to the Mg^{2+} ion and a water molecule hydrating the SO_4^{2-} ion. For $MgSO_4$ $N_{\vec{p}} = 18$, which is much larger than the sum of the hydration numbers of $Mg(ClO_4)_2$ and Cs_2SO_4 (see Fig.). This means that the dynamics of a large number of water molecules are affected, due to a cooperative effect of the cation and the anion. The size of most ions allows them to be structurally surrounded by 4-6 water molecules. Hence, a value of $N_{\vec{p}} > 6$ and $N_{\vec{\mu}} > 12$ implies that the effect of the ion on the orientational dynamics of water extends well beyond the first structurally surrounding shell of water molecules.

The same cooperativity is observed in the fs-IR measurements (see Fig.), where $MgSO_4$ has a much larger fraction of slowly reorienting water molecules (corresponding to a hydration number $N_{\vec{\mu}} = 32$) than $Mg(ClO_4)_2$ and Cs_2SO_4 (with hydration numbers $N_{\vec{\mu}}$ of 4 and 9, respectively). For $MgSO_4$, there are approximately twice as many slowly rotating OH-groups ($N_{\vec{\mu}}$) as slowly rotating dipoles ($N_{\vec{p}}$), indicating that the same collection of slow water molecules is observed by fs-IR and THz DR. Even the combination of the moderately strongly hydrated cation Na^+ with the strong anion SO_4^{2-} is observed to affect the dynamics of a large number of water molecules ($N_{\vec{\mu}} = 24$; see Fig. D). Thus the effects of ions and counterions can be strongly interdependent and non-additive. The key parameter determining how strongly ions affect water dynamics is thus the combination of the solvated cation and anion.

It is clear that the effect of $MgSO_4$ and Na_2SO_4 on water extends well beyond the first solvation shell of the ions and that the ions show strong cooperativity in affecting the dynamics of water molecules. It should be noted that this effect is not related to ion pairing. Previous GHz DR studies by Buchner et al. showed the presence of a certain amount of (single and double solvent separated) ion pairs for solutions of $MgSO_4$ and Na_2SO_4 [18, 20]. Ion pairs lead to additional resonances at very low frequencies (<5 GHz), located well outside our THz DR measurement window (0.4 - 1.2 THz). For our fs-IR measurements we can also neglect the direct contribution of ion pairs to the anisotropy data, since this technique excites and probes specifically the hydroxyl vibrations of water molecules. Hence, the dramatic slowing down

of the anisotropy decay for $MgSO_4$ and Na_2SO_4 corresponds to slow reorientation of water molecules, not the slow reorientation of ion pairs. A remaining question is whether the observed slow water molecules could be water hydrating ion pairs. This is in fact very unlikely because the amount of ion pairing is generally small - less than 10% for $MgSO_4$, even at high salt concentrations [18] - whereas the observed cooperative effect leads to a slowing down of a large fraction of the water (up to 70% of all water molecules in the solution; see Fig. D). Hence the slow water fraction is associated with hydration of non-paired Mg^{2+} and SO_4^{2-}.

The cooperativity in ion hydration can be explained from the fact that the cation and anion lock different degrees of freedom of the water molecules, i.e. the direction of the bisectrix ($\vec{p}$) and the direction of OH ($\vec{\mu}$), respectively. The nearby presence of both ions can thus lead to a locking in both directions of the hydrogen-bond structure of several intervening water layers, giving rise to the observation in DR and fs-IR of slowed down water molecules well beyond the first solvation shell. This cooperativity is schematically illustrated in Fig. 3C. As illustrated in this figure, we expect the solvation structures to be quite directional in between the ions. If an ion forms ∼4 of these structures with surrounding counterions, the value of $N_{\vec{p}}$ of 18 implies that each of these structures consist, on average, of 4-5 water molecules. This interpretation also means that for solutions like $MgSO_4$ and Na_2SO_4 the slowly reorienting water molecules are not arranged in a spherically symmetric way around the ions.

The reorientation of water molecules in the rigid, locked hydrogen bond structure occurring for $MgSO_4$ can be expected to show a different temperature dependence compared to pure liquid water. We measure the temperature dependence of the anisotropy decay for 1.5 mol/kg $MgSO_4$ (Fig. A) over an interval of about 50°C. We compare the temperature dependence to that of a 4 mol/kg Cs_2SO_4 solution (Fig. B) with the same hydration level (Fig. D), but no cooperativity. At room temperature, the anisotropy for $MgSO_4$ decays more slowly than for Cs_2SO_4, but with increasing temperature the situation reverses. To quantify the results, we fit the anisotropy data at different temperatures with a single averaged time scale for all water molecules in the system. This means that a change in this time scale represents both the changes in time scales and changes in the relative fractions of bulk-like and slow water molecules. Figure C shows a much stronger temperature dependence of this average time scale for a solution of 1.5 m $MgSO_4$ than for a solution of 4 m Cs_2SO_4.

The difference in temperature dependence of the reorientation of $MgSO_4$ and Cs_2SO_4 solutions indicates that the reorientation within the hydration structures involves a different mechanism. For pure water it was found from MD simulations that the reorientation of water follows a concerted mechanism and that the
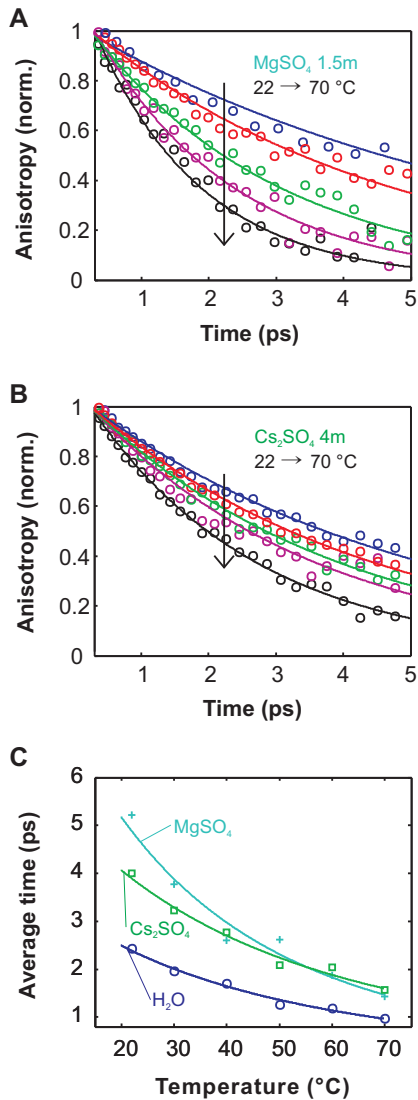
FIG. 4: Temperature dependence of the reorientation. The temperature dependent anisotropy decay data for MgSO$_4$(**A**) and Cs$_2$SO$_4$(**B**) with fits as explained in the text. **C** Average reorientation times of solutions of 1.5 mol/kg MgSO$_4$, 4 mol/kg Cs$_2$SO$_4$ and neat HDO:H$_2$O (from Ref. [26]) as a function of temperature.

rate-limiting step for reorientation of a water molecule is the motion of a second water molecule in and out of the solvation shell of the first [29, 30]. For the Cs$_2$SO$_4$ solution the hydration number $N_{\vec{\mu}}$ has a value of 9, which is likely associated with the OH groups of water molecules that are hydrogen bonded to the SO$_4^{2-}$ ion. In view of the small value of $N_{\vec{\mu}}$, these water molecules are surrounded by water molecules that show bulk-like dynamics. Hence, although the reorientation of the water molecules hydrating the SO$_4^{2-}$ is slow, the temperature dependence of this reorientation is similar to that of pure liquid water, because the reorientation is governed by hydrogen-bond interactions to water molecules that show bulk-like behavior. Correspondingly, the temperature dependence of the reorientation time of Cs$_2$SO$_4$ has the same slope as for bulk water In contrast, for MgSO$_4$ the solvation structures are large, as expressed by the large values of the hydration numbers $N_{\vec{p}} = 18$ and $N_{\vec{\mu}} = 32$. Hence, the reorientation of a water molecule in the solvation structure relies on the motions of water molecules that are contained in the same solvation structure. These motions are substantially slowed down, and reorientation thus involves a collective reorganization of the extended solvation structure, which explains the difference in temperature dependence with a solution of Cs$_2$SO$_4$ and pure liquid water.

In conclusion, we have found that the hydration structure of a strongly hydrated ion depends critically on the nature of its counterion. If the counterion is weakly hydrated, the strongly hydrated ion is surrounded by a semi-rigid solvation shell, where reorientation is restricted only in a certain direction, but is still allowed in other directions. If, however, strongly hydrated cations and anions are combined, the dynamics of water molecules well beyond the first solvation layer are affected. In this case, the hydrogen bond network is locked in multiple directions. These findings show that the effect of ions on water dynamics can be strongly interdependent and non-additive.

[1] W. Kunz, J. Henle and B.W. Ninham, Curr. Opin. Colloid Interface Sci. **9**, 19 (2004)
[2] P. Jungwirth and Tobias, D.J., Chem. Rev. **106**, 1259 (2006)
[3] Y. Marcus, Chem. Rev. **109**, 1346 (2009)
[4] D.J. Tobias and J.C. Hemminger, Science **319**, 1197 (2008)
[5] F. Franks. Ed., *Water: A Comprehensive Treatise* (Plenum, New York, 1973)
[6] R. Mancinelli et al., J. Phys. Chem. B **111**, 13570 (2007)
[7] K.D. Collins, G.W. Neilson and J.E. Enderby, Biophys. Chem. **128**, 95 (2007)
[8] C. D. Cappa et al., J. Phys. Chem. B **110**, 5301 (2006)
[9] J.D. Smith, R.J. Saykally and P.L. Geissler, J. Am. Chem. Soc. **129**, 13847 (2007)
[10] A.W. Omta et al., Science **301**, 347 (2003)
[11] S. Park and M.D. Fayer, Proc. Nat. Ac. Sci. USA **104**, 16731 (2007)
[12] D.E. Moilanen et al., Proc. Nat. Ac. Sci. USA **106**, 375 (2009)
[13] D.A. Turton et al., J. Chem. Phys. **128**, 161102 (2008)
[14] U. Kaatze, J. Solution Chem. **26**, 1049 (1997)
[15] R. Buchner, G.T. Hefter and P.M. May, J. Phys. Chem. A **103**, 1 (1999)
[16] T. Chen, G. Hefter and R. Buchner, J. Phys. Chem. A **107**, 4025 (2003)

[17] W. Wachter et al., J. Phys. Chem. A **109**, 8675 (2005)

[18] R. Buchner, T. Chen and G. Hefter, J. Phys. Chem. B **108**, 2365 (2004)

[19] W. Wachter et al., J. Phys. Chem. B **111**, 9010 (2007)

[20] R. Buchner et al., J. Phys Chem B **103**, 1185 (1999)

[21] J.T. Kindt and C.A. Schmuttenmaer, J. Phys. Chem. **100**, 10373-10379 (1996)

[22] C. Rønne et al., J. Chem. Phys. **107**, 5319 (1997)

[23] D. Laage and J.T. Hynes, Proc. Nat. Ac. Sci. USA 104, 11167 (2007)

[24] Y.S. Lin, B.M. Auer, J.L. Skinner, J. Chem. Phys. **131**, 144511 (2009)

[25] Y.L.A. Rezus and H.J. Bakker, J. Chem. Phys. **123**, 114502 (2005)

[26] K.J. Tielrooij et al., Chem. Phys. Lett. **471**, 71 (2009)

[27] S. Koneshan et al., J. Phys. Chem. B **102**, 4193 (1998)

[28] H. Ohtaki and T. Radnai, Chem. Rev. **93**, 1157 (1993)

[29] D. Laage and J.T. Hynes, Science **311**, 832-835 (2006)

[30] D. Laage and J.T. Hynes, J. Phys. Chem. B **112**, 14230 (2008)

[31] C.J.F. Böttcher, *Theory of Electric Polarization*, Elsevier (Amsterdam), Vol I, 1973

[32] C.J.F. Böttcher, *Theory of Electric Polarization*, Elsevier (Amsterdam), Vol II, 1978

[33] C. Ronne, P.O. Astrand, S.R. Keiding, Phys. Rev. Lett. **82**, 2888 (1999)

[34] T. Fukasawa et al., Phys. Rev. Lett. **95**, 197802 (2005)

[35] H. Yada, M. Nagai and K. Tanaka, Chem. Phys. Lett. **464**, 166 (2008)

[36] J.B. Hubbard et al., Proc. Nat. Acad. Sci. USA **74**, 401 (1977)

[37] Y. Hayashi et al., J. Phys. Chem. B **111**, 1076 (2007)

[38] H. Bianchi, H.R. Corti and R. Fernández-Prini, J. Sol. Chem. **17**, 1059 (1988)

[39] K.J. Tielrooij et al., Phys. Rev. Lett. **102**, 198303 (2009)

[40] S. Woutersen and H.J. Bakker, Nature 402 (1999), 507

[41] P.-Å. Bergström, J. Lindgren and O. Kristiansson, J. Phys. Chem. 95, 8575 (1991)

[42] M.F. Kropman and H.J. Bakker, Science **291**, 5511 (2001)

[43] M.F. Kropman, H.-K. Nienhuys and H.J. Bakker, Phys. Rev. Lett. **88**, 077601 (2002)

[44] C. Akilan et. al., ChemPhysChem. **7**, 2319 (2006)

[45] P. Van Rysselberghe and J. M. McGee, J. Am. Chem. Soc., **65**, 737 (1943)

[46] This work is part of the research program of the "Stichting voor Fundamenteel Onderzoek der Materie (FOM)", which is financially supported by the "Nederlandse organisatie voor Wetenschappelijk Onderzoek (NWO)". The authors thank H. Schoenmaker for technical support and R.L.A. Timmer and E.H.G. Backus for useful discussions and D. Frenkel and E.W. Meijer for helpful comments on the manuscript.

A1. APPENDIX

A2. TERAHERTZ DIELECTRIC RELAXATION SPECTROSCOPY

Method

We perform dielectric relaxation (DR) spectroscopy using a terahertz time-domain spectroscopy (THz-TDS) setup. This setup is based on THz generation and detection in ZnTe non-linear crystals, using 800 nm pulses with a duration of ∼150 fs. The time dependent electric field strengths of the THz pulses (∼1 ps) that are transmitted through the sample are measured by means of electro-optic sampling with a variably delayed pulse of 800 nm light with a duration of ∼150 fs in the second ZnTe crystal. By comparison of the THz pulse that is transmitted through an empty cuvette and through a cuvette filled with the sample, we can extract the complex refractive index $\hat{n} = n + ik$. Here n is the regular refractive index and k is the extinction coefficient. We follow the convention of discussing the complex dielectric function $\hat{\epsilon} = \hat{n}^2$, in the case of aqueous samples. We determine the frequency-dependent complex dielectric response $\hat{\epsilon}(\omega)$ for a number of salts in solution. Each measurement consists of a sample, which is measured quasi-simultaneously with a reference sample. We measure the following combinations of salt solutions: $MgCl_2$-CsCl, LiCl-CsCl, Cs_2SO_4-CsCl, $Mg(ClO_4)_2$-CsCl and $MgSO_4$-Cs_2SO_4. In most cases, the salt CsCl is chosen as a reference sample, since its dielctric properties are known and the ions Cs^+ and Cl^- have a negligible hydration effect according to GHz dielectric relaxation measurements [16]. We have measured other additional combinations of samples and reference samples, to assure consistency. We compare samples with the same amount of water in each sample, i.e. by using molality (mol/kg). We employ a mechanical device that alternatively positions the sample and the reference sample (contained in cuvettes that have chambers with an optical path length of 103 ± 0.5 μm) in the THz beam. This approach minimizes the effect of fluctuations in THz intensity and temperature as noise sources. A schematic overview of the setup is given in Fig. A1.

Modeling

Molecular reorientation processes lead to dielectric relaxation, i.e. the anomalous dispersion of the dielectric constant and the accompanying absorption of electromagnetic energy [31]. An electric field applied to water molecules will tend to align the permanent dipoles $\overrightarrow{p}$ associated with the water molecules, resulting in an induced polarization $\overrightarrow{M} = \Sigma \overrightarrow{p} = (\epsilon - 1)\epsilon_0 \overrightarrow{E}$, where ϵ is the dielectric function and ϵ_0 is the vacuum permittivity.
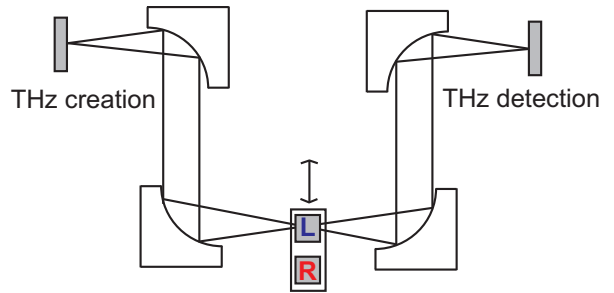

FIG. A1: The THz-TDS setup that we use to perform differential dielectric relaxation measurements on two samples that are probed alternatively. The grey blocks are the ZnTe crystals and L and R indicate the sample positions.

If the electric field is oscillating, the water molecules reorient to align their dipole moments with the driving field. When the angular frequency ω of an oscillating electric field becomes higher than the reciprocal reorientation time, the real part of the complex dielectric function $\hat{\epsilon}(\omega)$ drops, because the water molecules can not reorient fast enough to align with the externally applied electric field. The imaginary part of $\hat{\epsilon}(\omega)$ shows an absorption peak around the reciprocal reorientation time. Hence, the frequency dependence of the dielectric response contains information about the reorientation dynamics of water molecules.

The dielectric response of pure water has shown evidence for two molecular reorientation processes [21, 22, 33–35]. The process with the largest strength is associated with the cooperative reorganization of water molecules, which occurs on the Debye timescale, $\tau_D \approx 8$ ps in pure water at room temperature. A second reorientation process with a smaller strength is generally associated with the reorientation of undercoordinated water molecules and has a typical timescale of $\tau_2 \approx 250$ fs. We model the dielectric response of ionic solutions, using a double-Debye model that accounts for the two molecular reorientation processes with an additional term for the ion conductivity σ:

$$\hat{\epsilon}(\omega) = \frac{S_1}{1 + i\omega\tau_D} + \frac{S_2}{1 + i\omega\tau_2} + \frac{\sigma}{i\omega\epsilon_0} + \epsilon_\infty. \quad (A1)$$

Here, the first term represents the relaxation process with timescale τ_D and amplitude S_1. The second term represents the relaxation process with timescale τ_2 and amplitude S_2. In the case of pure water at room temperature, $S_1 \approx 75$ and $S_2 \approx 1.8$ [35]. The dielectric constant in the high frequency limit is given by ϵ_∞.

The third term due to ion conductivity is not the only effect of ions on the dielectric response, since ions can affect the structure and dynamics of the surrounding water molecules. Solvated ions may affect the Debye time τ_D and the strength of the relaxation process S_1

of the water molecules in the solution. The effect of solvated ions on the Debye time τ_D of water molecules is expressed in the lowering of τ_D with increasing ion concentration ($\sim$10 % for a 1 molar solution). It was found that this effect has a negligible dependence on the nature of the ions [16, 17, 19]. Concerning the effect of ions on the relaxation strength S_1, there are three effects that can lead to a lowering of S_1, i.e. depolarization: *i)* due to the presence of ions, the solution's water concentration is slightly lower than the pure water case, resulting in a small overall lowering of the dielectric response; *ii)* due to strong (irrotational) bonding of a number of water molecules in the vicinity of ions, these water molecules can no longer participate in the relaxation process with τ_D; and *iii)* due to ions that move in the driving field, water molecules are caused to reorient in a direction opposite to the driving field (kinetic depolarization) [14, 36].

The depolarization effect can be used to extract the ion's hydration number, defined as the number of water molecules around an ion that are strongly bound and no longer participate in dielectric relaxation due to the presence of the ion (effect *ii* mentioned above). This has been done successfully for a large number of ionic solutions by Buchner et al. [15–20]. In order to extract the hydration number, we first correct the depolarization effect of an ion ΔS_1 for the effect of kinetic depolarization (effect *iii* mentioned above), which is proportional to the conductivity and depends on the concentration c of the solution [14, 15]:

$$\Delta S_{1,\text{kin.dep.}}(c) = \sigma(c) \cdot \frac{2\tau_D(0)}{3} \frac{\epsilon(0) - \epsilon_\infty(c)}{\epsilon(0)\epsilon_0}. \quad \text{(A2)}$$

After having corrected the depolarization ΔS_1 for the kinetic depolarization, we obtain the corrected depolarization $\Delta S_1'$. This number is negative, since it is a reduction of the induced polarization, and can be translated into the hydration number N, using [37]

$$N(c) = \left(c_s - \frac{S_1 + S_2 + \Delta S_1'}{S_1 + S_2}c_0\right)/c \quad \text{(A3)}$$

In this equation, S_1 and S_2 are the relaxation strengths in pure water, c_s is the concentration of solvent water molecules in the solution and c_0 represents the concentration of water molecules of pure water. Here, the dilution effect of the ionic solution (effect *i* mentioned above) is taken into account through the concentrations c, c_s and c_0.

For each measurement where we compare two different salts, we use literature data to reduce the number of fit parameters. We use the parameter S_1 for the reference salt solution of CsCl from Ref. [16] and literature values for the ion conductivities of the solutions CsCl, $MgCl_2$, LiCl, Cs_2SO_4, $MgSO_4$ and $Mg(ClO_4)_2$ from

Refs. [16, 18–20, 38, 44, 45]. Finally, for each sample, we fix τ_D to the value that was found for the accompanying reference sample. The same fitting constraints have been applied previously to measurements of different acid-salt combinations and yielded consistent results for the hydration of protons [39].

A3. FEMTOSECOND INFRARED SPECTROSCOPY

Method

The setup used for measuring the molecular reorientation dynamics employs a commercial Ti:sapphire regenerative amplified laser system (Spectra-Physics Hurricane) that delivers 800 nm pulses with a duration of $\sim$100 fs with an energy of 1 mJ at a rate of 1 kHz. Part of this light is used to pump a white-light seeded optical parametric amplifier (OPA) based on a β-barium borate (BBO) crystal. The idler output from the OPA, with a wavelength of 2 μm, is frequency doubled in a second BBO crystal to 1 μm and then difference-frequency mixed with the remaining 800 nm light from the amplifier in a potassium niobate crystal. This produces $\sim$5 μJ of 4 μm light with a pulse duration of $\sim$150 fs. The absorption peak of the OD-stretch vibration in pure D_2O:H_2O is around 2500 cm^{-1}. However, we tune the center frequency to $\sim$2430 cm^{-1} to preferentially pump and probe water molecules with a red-shifted OD-stretch frequency and to exclude blue-shifted OD-stretch frequencies, which correspond to weakly bonded water molecules trypically found surrounding certain anions.

The pump-probe experiment is conducted by sending part of the 4 μm light into the pump branch and part into the probe branch of the set-up. The pump and probe pulses are focused on the same spot in the sample. Every other pump pulse is blocked by a 500 Hz laser-synchronized chopper, so that every consecutive probe pulse experiences either an excited or a non-excited sample. The difference between these consecutive signals gives the pump-induced change in absorption of the sample $\Delta\alpha$. A reference pulse that is focused on a different spot on the sample allows compensation for fluctuations in the probe intensity. The absorption of the probe pulse and the reference pulse is measured with a 2×32 liquid-nitrogen cooled mercury-cadmium-telluride (MCT) array spectrometer, resulting in $\Delta\alpha(\omega)$. A delay stage that controls the relative delay between pump and probe pulse is used to monitor the dynamics of the pump-induced change in absorption $\Delta\alpha(\omega,t)$, where t is the pump-probe delay time. To measure reorientation dynamics, a $\lambda/2$-plate is placed in the pump path in combination with a motor-controlled polarizer in the probe path after the sample. This makes it possible to

Modeling

From our measurements we obtain the pump-induced absorption change as a function of frequency and pump-probe delay for parallel ($\Delta\alpha_\parallel$) and perpendicular polarization ($\Delta\alpha_\perp$). We use $\Delta\alpha_\parallel$ and $\Delta\alpha_\perp$ to construct the isotropic signal, which is independent of reorientation:

$$\Delta\alpha_{\text{iso}} = \frac{1}{3}(\Delta\alpha_\parallel + 2\Delta\alpha_\perp). \qquad (A4)$$

To obtain the anisotropy dynamics of the excited OD-stretch dipole vectors, the measured data $\Delta\alpha_\parallel$ and $\Delta\alpha_\perp$ are corrected for the time-dependent thermalization signal. The temporal evolution of this contribution to the signal can be obtained from a detailed investigation of the isotropic signal. All data are modeled with the energy relaxation model described in ref [25]. In this model the energy from the OD-stretch vibration is transferred through an intermediate state (presumably the bending mode) to a thermal end level (lower energy modes). The model contains two main fit parameters: τ_1 (first excited state OD-stretch $\rightarrow$ intermediate state) and τ^* (intermediate state $\rightarrow$ thermal end state). A least squares fit is conducted for the whole spectrum at each delay time to find the two timescales that constitute the best fit. The heated end spectrum corresponds well with the difference of the absorption of a slightly heated sample and a sample at ambient temperature.

In figure A2, we show the results of our fitting procedure for the different salt solutions. Clearly, the salts that contain sulfate do not give rise to increased excited state lifetimes. Previous fs-IR measurements of reorientation of water around the anions I$^-$, Cl$^-$ and Br$^-$ [10, 42, 43] have shown a significant slow reorientation component. For the anions I$^-$, Cl$^-$ and Br$^-$ the reason for this could be that the measurement technique preferentially monitors intact OD-anion bonds, due to the longer vibrational lifetime. Hence, after a long pump-probe delay time, only OD bonds that are still hydrogen-bonded to the anion are probed, which obviously have intact hydrogen bonds with the anion [23]. However, the case of sulfate anions is different, since there is no increase of the vibrational lifetime. Therefore in this case, there is no preference for measuring OD-bonds that have not reoriented. Since we still observe a clear increase in the reorientation time, this means that water around SO$_4^{2-}$ inherently reorients more slowly.

We use the heat-corrected data $\Delta\alpha'_\parallel$ and $\Delta\alpha'_\perp$ to construct the anisotropy $R(t)$, where t is the pump-probe delay time:

$$R = \frac{\Delta\alpha'_\parallel - \Delta\alpha'_\perp}{\Delta\alpha'_\parallel + 2\Delta\alpha'_\perp}. \qquad (A5)$$

detect the induced absorption for a probe polarization parallel to the pump polarization ($\Delta\alpha_\parallel$) and the signal measured with a probe polarization perpendicular to the pump ($\Delta\alpha_\perp$).

The samples consist of different salts that are solvated in a mixture of 4% D$_2$O in H$_2$O. In these isotopically diluted samples, resonant energy transfer (Förster transfer), which leads to a fast orientational randomization ($<$ 100 fs [40]), is avoided. The samples are placed between two CaF$_2$ windows that are separated by a 25 μm spacer. We investigate the following salt solutions: Mg(ClO$_4$)$_2$, LiI, MgSO$_4$, Na$_2$SO$_4$ and Cs$_2$SO$_4$. We use the anions ClO$_4^-$ and I$^-$ because they form very weak hydrogen bonds and result in an anionic solvation layer with water molecules that have a blue-shifted OD-stretch frequency [41, 43]. The absorption band of these anion-bound water molecules is well-separated from that of the other water molecules, thus allowing the selective excitation and probing of water molecules in different environments.
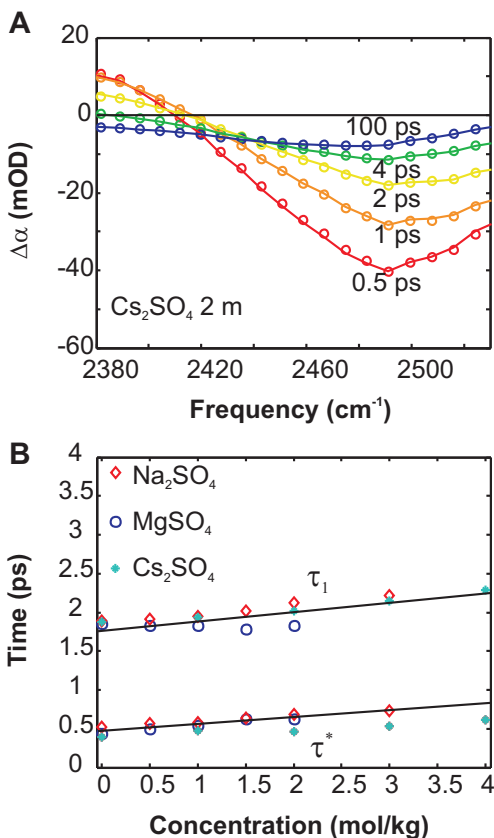

FIG. A2: A typical pump-induced absorption spectrum for a number of pump-probe delay times for a 2 m solution of Cs$_2$SO$_4$ (**a**). Figure **b** gives the fit results for the timescales τ_1 and τ^* as a function of ion concentration, after modeling the energy relaxation. The lines are guides to the eye.
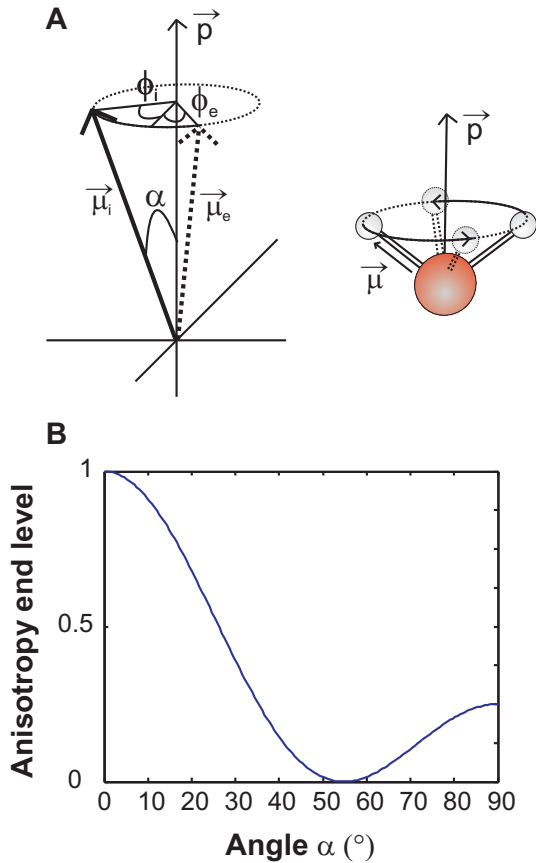
FIG. A3: a Graphical representation of the geometry, where a water molecule can rotate around the axis of its permanent dipole $\vec{p}$. The initial and final state of the OD-stretch dipole moment are given by $\vec{\mu}_i$ and $\vec{\mu}_e$, respectively. **b** The anisotropy end level is given as a function of the angle α between $\vec{\mu}$ and the axis of rotation.

The anisotropy is proportional to the second order orientational correlation function $R(t) = \frac{2}{5}C^{(2)}(t)$, where

$$C^{(2)}(t) = \left\langle P_2[\vec{\mu}_i(0) \cdot \vec{\mu}_i(t)]\right\rangle \propto e^{-t/\tau_r} \quad . \quad \text{(A6)}$$

Here $P_2[x]$ is the second order Legendre polynomial in x, $\vec{\mu}_i(t)$ is the OD-stretch transition dipole

moment of the ith molecule at time t and τ_r denotes the (second order) reorientation time. Eq. A6 shows that fs-IR probes the dynamics of individual water molecules. In dielectric relaxation measurements, the Fourier transform of the first order correlation function, $C^{(1)}(t) = \left\langle P_1[\vec{M}(0) \cdot \vec{M}(t)]\right\rangle$, is measured. Here P_1 is the first order Legendre polynomial and $\vec{M}(t)$ the total permanent dipole moment ($\vec{M} = \Sigma_i \vec{p}_i$) of the system at time t [32]. It has been shown that the reorientation time τ_r, as measured for a 4 % D_2O in H_2O solution, corresponds well to the Debye reorientation time τ_D for H_2O, corrected by a factor ~ 3 for a large range of temperatures [26].

Reorientation around a cone

We calculate the expected end level of the anisotropy $R_{t\to\infty}$ for a water molecule that can rotate with a fixed angle around an axis. The geometry is given in Fig. A3a, where it is generalized to the rotation of a vector around an axis with an angle α between vector and axis. The initial orientation μ_i corresponds to an angle ϕ_i in the circular plane in which the vector will precess. The final orientation is associated with angle ϕ_e. We take $\phi_i = 0$ and integrate over ϕ to allow the final orientation to have a randomly distributed angle $\phi = \{0, 2\pi\}$. We find

$$R_{t\to\infty} = \frac{2}{5}\int_0^{2\pi} P_2(\mu_i \cdot \mu_e)d\phi. \quad \text{(A7)}$$

with $P_2(x) = \frac{1}{2}(3x^2 - 1)$, the second order Legendre polynomial, $\mu_i = (\sin(\alpha), 0, \cos(\alpha))$ and $\mu_e = (\sin(\alpha)\cos(\phi), \sin(\alpha)\sin(\phi), \cos(\alpha))$. The result for the anisotropy end level is shown in Fig. A3b as a function of angle α. The angle between the rotating vector and the rotational axis in the case of a water molecule that rotates around its permanent dipole is half the DOH bond angle and hence $\sim 52°$. It is clear that the anisotropy end level is very small (< 0.005).